Discovery of indoline derivatives that inhibit esophageal squamous cell carcinoma growth by Noxa mediated apoptosis

Dong-Jun Fu[a,b,c,1], Miaomiao Li[a,1], Sai-Yang Zhang[a,d,1], Jiang-Feng Li[a], Beibei Sha[a], Longhao Wang[a], Yan-Bing Zhang[b,c], Ping Chen[a,d,*], Tao Hu[a,*]

[a] *School of Basic Medical Sciences, Zhengzhou University, Zhengzhou 450001, China*
[b] *New Drug Research & Development Center, School of Pharmaceutical Sciences, Zhengzhou University, Zhengzhou 450001, China*
[c] *Collaborative Innovation Center of New Drug Research and Safety Evaluation, Zhengzhou 450001, China*
[d] *Henan Institutes of Advanced Technology, Zhengzhou University, Zhengzhou 450001, China*

A B S T R A C T

A series of novel indoline derivatives were synthesized and evaluated for antiproliferative activity against four selected cancer cell lines (Hela, A549, HepG2 and KYSE30). Among them, compound **20** displayed the potent inhibition activity against esophageal cancer cells (Kyse30, Kyse450, Kyse510 and EC109). Cellular mechanism studies in esophageal squamous cell carcinoma (ESCC) cells elucidated compound **20** inhibited cell growths *in vitro* and *in vivo*, reduced colony formation, arrested cell cycle at M phase, and induced Noxa-dependent apoptosis in ESCC. Importantly, compound **20** was identified as a novel Noxa mediated apoptosis inducer. These results suggested that compound **20** might be a promising anticancer agent with potential for development of further clinical applications.

1. Introduction

Heterocycle-fused scaffolds as one of the privileged structures in drug discovery exhibit various biological activities allowing them to act as anticancer, antiinflammatory, antipsychotic, and antidiabetic agents [1–7]. Indoline as a simple class of heterocycle-fused scaffold prolifically designed with strong pharmacological significances in particular of anticancer ability [8–10]. 1-Aroylindoline-hydroxamic acid **1** (Fig. 1) as a dual HDAC6/HSP90 inhibitor displayed striking cytotoxic effects with GI_{50} values ranging 1.04–1.61 μM against lung A549, colon HCT116 and leukemia HL60 cell lines [11]. Indoline **2** demonstrated the significantly anticancer activity in a UACC-62 xenograft model in mice [12]. 7-Aroyl-aminoindoline-1-sulfonamide **3** inhibited the human cancer cell growth of gastric MKN45, lung H460, and colon HT29 cells with an IC_{50} value of 8.8, 9.4, and 8.6 nM, respectively [13]. Indoline-pyrimidine hybrid **4** could inhibit protein kinase R-like endoplasmic reticulum kinase (PERK) activation and suppress the growth of a human tumor xenograft in mice [14]. 1-Arylsulfonyl indoline **5** exhibited the potent antiproliferative activity against lung A549 cells with an IC_{50} value of 79 nM [15]. Compound **6** could inhibit multidrug resistant cancer cell lines and arrest cell cycle at G2/M phase [16]. 1-(Sulfonyl)-5-(arylsulfonyl)indoline **7** was designed and synthesized as a activator

of the tumor cell specific M2 isoform of pyruvate kinase [17]. Spirooxindole derivative **8** caused restoration of the tumor protein 53 function by triggering its nuclear accumulation and preventing its proteasomal degradation as an anti-breast cancer agent [18]. Indoline analogue **9** as a novel receptor-interacting protein kinase 1 inhibitor exhibited the potent antimetastasis activity in the experimental B16 melanoma lung metastasis model [19].

As one of the most aggressive digestive system tumors, esophageal squamous cell carcinoma is associated with numerous factors, including advanced age, achalasia, tobacco use, alcohol abuse, high-starch diets lacking in fruits, and so on [20–22]. In 2012, 400,000 deaths were reported in the world due to esophageal carcinoma [23]. Chemical prevention and treatment using synthetic drugs has emerged as an advanced strategy for esophageal squamous cell carcinoma [24–26]. Noxa as a B-cell lymphoma 2 (Bcl-2) family member plays an important role in apoptosis induction [27]. Activated Noxa could inhibit the activities of Bfl-1/A1 and Mcl-1, then release and directly bind Bak and Bax to promote cell apoptosis [28]. So, Noxa might be a promising target for developing new chemotherapeutic agents to treat esophageal carcinoma.

Here, a series of new anticancer indolines were synthesized and explored for their antiproliferative activity. In order to investigate the
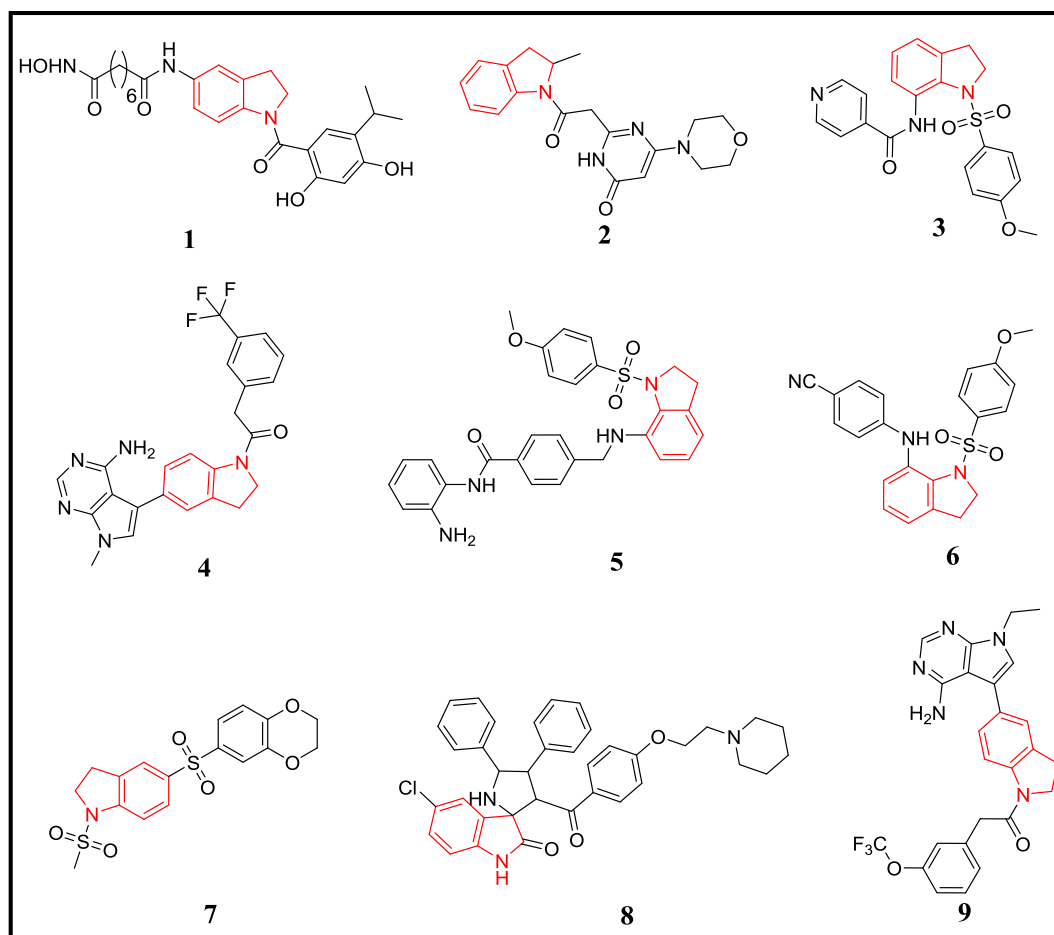

Fig. 1. The chemical structures of anticancer indolines.

broad-spectrum anti-cancer activity, four different cancer cell lines (Hela, A549, HepG2 and KYSE30) were selected to obtain IC_{50} values. Importantly, the anticancer mechanisms *in vitro* and *in vivo* against esophageal squamous cell carcinoma of indolines were evaluated.

2. Results and discussion

2.1. Chemistry

The synthetic route of indoline derivatives were shown in Scheme 1. 5-(Bromomethyl)-1,2,3-trimethoxybenzene **11** was synthesized by reacting (3,4,5-trimethoxyphenyl)methanol **10** with phosphorus tribromide in the chloroform system according to previous references [29–31]. With the intermediate **11** in hand, we next synthesized indoline derivatives bearing a 3,4,5-trimethoxyphenyl scaffold **12–13** by the nucleophilic substitution reaction. Treatment of substituted benzoyl chloride and thiophene-2-carbonyl chloride with aromatic amine in the presence of sodium hydroxide furnished indoline derivatives **15–17** and **29–32**. The structure confirmation of all indoline derivatives were described in the Supporting Information.

2.2. Antiproliferative activity of indoline derivatives

In order to discovery novel Noxa mediated apoptosis inducers, we evaluated the antiproliferative activity of all indoline derivatives against Hela (Human cervical cancer cell line), A549 (Human lung carcinoma cell line), HepG2 (Human liver cancer cell line), and KYSE30 (Human esophagus cancer cell line) using the CCK8 assay. In this paper, the anticancer drug **5-FU** was used as the reference drugs in the CCK8

assay [32–36]. Representative chemical features of indoline derivatives are the 3,4,5-trimethoxyphenyl moiety linked to a substituted indoline ring through a carbonyl and methylene group spacer (Fig. 2). On the basis of that scaffold, we designed different structures depicted in Fig. 2 to determine the relationship between chemical structures and antiproliferative activity. Several substituents such as bromine atom, nitro, or methyl were introduced in the heterocycle core or the indoline ring. Moreover, the influence of the nature of the heterocyclic moiety in antiproliferative activity was studied. Thus, the indoline scaffold was changed by indole, phenothiazine, 1,2,3,4-tetrahydroquinoline, and 2,3,4,5-tetrahydro-1*H*-benzo[*b*]azepine. Finally, the importance of 3,4,5-trimethoxyphenyl moiety was also analyzed.

The carbonyl and methylene group spacer between 3,4,5-trimethoxyphenyl moiety and indoline ring affected the antiproliferative activity against four cancer cell lines. When the methylene group was replaced by a carbonyl group, the antiproliferative activity against Hela, A549 and KYSE30 cells were improved (**12** *Vs* **15**, **13** *Vs* **16**). Data collected in Table 1 show that the inhibitory potency against Hela and A549 cells is decreased when the indoline ring was replaced by a 1,2,3,4-tetrahydroquinoline ring or 2,3,4,5-tetrahydro-1*H*-benzo[*b*] azepine ring, indicating that the size of indoline ring played an important role for antiproliferative activity. Especially, indoline **16** displayed the potent activity against Hela, A549, HepG2 and KYSE30 cells with IC_{50} values of 4.32 μM, 18.41 μM, 23.72 μM and 12.76 μM, respectively.

Modification of the nature of the heterocyclic moiety present in the target analogues by introduction of indole (compound **18**) or phenothiazine (compound **19**) led to potent activity results against four cancer cell lines with IC_{50} values ranging from 1.35 μM to 19.45 μM. All
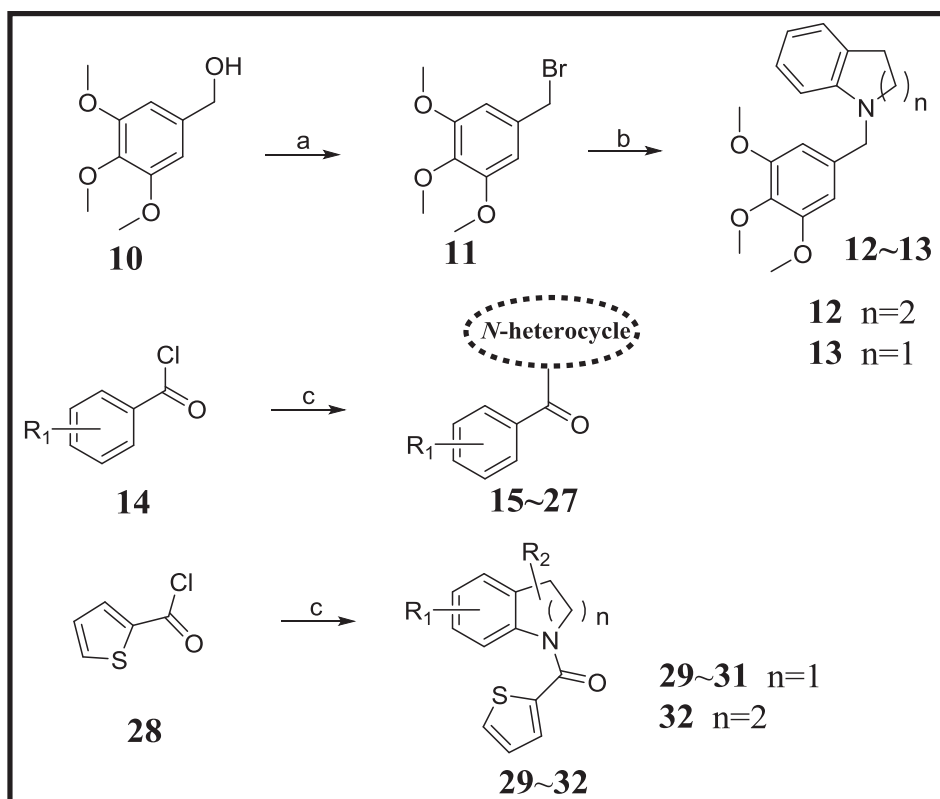
Scheme 1. Reagents and conditions: (a) PBr₃, CHCl₃, reflux; (b) K₂CO₃, aromatic amine, acetone, reflux; (c) Aromatic amine, K₂CO₃, acetone, reflux.
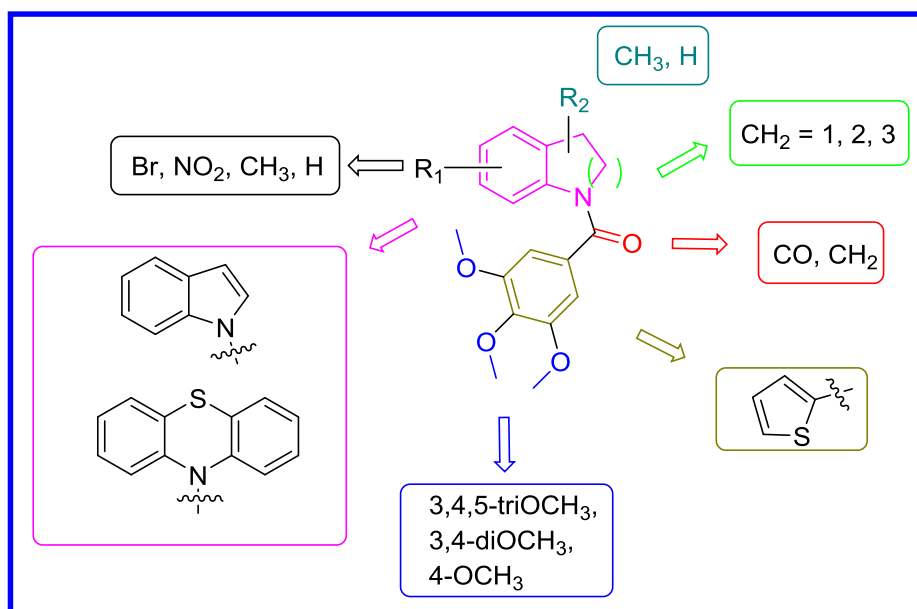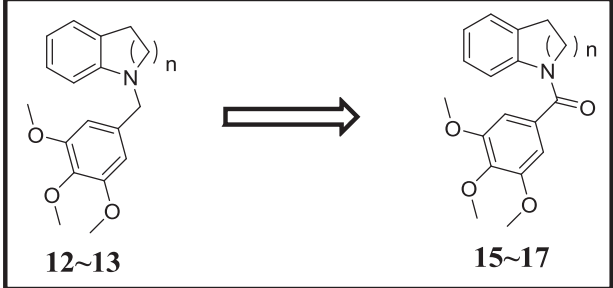

Fig 2. Structural modifications proposed from the hit indolines.

these results investigated that heterocyclic moiety palyed an important role for the antiproliferative activity. Several indoline-3,4,5-tri-methoxyphenyl derivatives were then prepared which incorporate diverse substituents in different positions of the indoline ring. One striking observation is the influence that the introduction of a bromine atom attaching to indoline ring of compound **20** in the inhibitory activity. When the hydrogen atom attaching phenyl ring of compound **16** was replaced by a bromine atom, compound **20** displayed more potent antiproliferative activity against A549, HepG2 and KYSE30 cells. These results indicated that the bromine atom as an electron-withdrawing

group might affect the inhibitory activity of indolines. In addition, the importance of 3,4,5-trimethoxyphenyl unit was explored. Target derivatives **24–27** without the 3,4,5-trimethoxyphenyl unit showed the weak activity results against A549 cancer cells with IC$_{50}$ values > 80 μM. However, target derivatives **18–23** with the 3,4,5-trimethoxyphenyl unit showed the potent activity results against same cancer cells A549 with IC$_{50}$ values < 20 μM (see Table 2).

To explore the effect of heterocycle for the inhibitory activity, thiophene was introduced into the targeted compounds **29–32**. A comparison with the antiproliferative activity results of compound **31**,

Table 1
Antiproliferative activity of the synthetic derivatives **12–13** and **15–17**.

Compound	n	IC$_{50}$ (μM)[a]			
		Hela	A549	HepG2	KYSE30
5FU	–	22.08 ± 0.05	4.22 ± 0.04	1.32 ± 0.04	1.46 ± 0.03
12	2	8.46 ± 0.04	> 80	8.09 ± 0.05	10.42 ± 0.04
13	1	5.98 ± 0.04	20.71 ± 0.08	3.61 ± 0.02	17.67 ± 0.11
15	2	7.57 ± 0.06	34.05 ± 0.05	13.73 ± 0.09	7.92 ± 0.03
16	1	4.32 ± 0.05	18.41 ± 0.08	23.72 ± 0.11	12.76 ± 0.07
17	3	> 80	31.38 ± 0.14	21.74 ± 0.07	6.55 ± 0.09

[a] Antiproliferative activity was assayed by exposure for 48 h. Data are presented as the means ± SDs from the dose-response curves of three independent experiments.

analogues **29** and **30** with substituents in the indoline ring exhibited better antiproliferative activity results against Hela cells and A549 cells. Replacing the indoline scaffold of **31** with 1,2,3,4-tetrahydroquinoline ring of **32** led to a decrease of the antiproliferative activity against the KYSE30 cells and an increase of the antiproliferative activity against the A549 cells. All these results suggested that the indoline ring with substituents played a significant role in their activities (see Table 3).

2.3. Biology mechanism

2.3.1. Compound 20 inhibited ESCC cell growth in vitro and in vivo

Indoline derivative compound **20** was chosen to do the further research, and four ESCC cell lines (Kyse30, Kyse450, Kyse510, EC109) were selected to test the inhibition activities against ESCCs of compound **20** *in vitro*. Compound **20** treatment showed a strong inhibition against the ESCCs in a concentration depend manner, the IC$_{50}$ values against cell lines were all less than 2 μM, presented in a dose-dependent manner (Fig. 3A). Results in Fig. 3B showed that as the concentration increased the cell colonies were evidently decreased by compound **20**, which illustrated compound **20** inhibited the colony formatting. To verify the consistency of results *in vitro* and *in vivo*, mice xenograft Kyse450 tumor model was established. Mice were treated for 30 days at dose of 150 mg/kg/day. As shown in Fig. 3B and D, the tumors had been significantly reduced by compound **20**. These data confirmed that the indoline **20** showed a high inhibition activity against ESCC cell lines *in vitro* and *in vivo*.

2.3.2. Compound 20 induced G2/M phase arrest

To test the effect of compound **20** on the cell cycle arrestment, cells' nucleus were stained with PI and analyzed by flow cytometry. As shown in Fig. 4A and B, the percentage of cells at G2/M phase was markedly elevated with the compound **20** treatment. For the Kyse30 and Kyse450 cell lines, 2.5 μM treatment up regulated G2/M percentage up to 4.9 times (Kyse30) and 6.1 times (Kyse450) comparing with control group.

Since the flow cytometry results cannot distinguish G2 or M arrestment, some G2/M phase related proteins were detected. In both Kyse30 and Kyse450 cells Wee1, p-Wee1, CDK1, Cyclin B1 and p-Histone H3 were up regulated as the concentration of compound **20** raises, which indicated the cell cycle arrestment caused by compound **20** is M phase arrestment (Fig. 4C).

2.3.3. Compound 20 induced cell apoptosis

Flow cytometry analysis was performed after the cells were treated with compound **20** and stained with Annexin V-FITC/PI to check the apoptosis induced by compound **20**. Results in Fig. 5 shows that compound **20** induced cell apoptosis in both Kyse30 and Kyse450 cell lines in dose depended manner. In both 2 cell lines, the apoptosis percentage rise to approximately 50% from control which is under 5% (Fig. 5A). The activation of Caspase-3 were enhanced by compound **20** treatment in both cell lines, Caspase-3 in about 45% cells has been activated (Fig. 5B). Similarly, compound **20** significantly induced the cleavage of Caspase-9, Caspase-3, and PARP (Fig. 5C). These results suggest that compound **20** triggered Caspases related apoptosis in ESCC cells.

2.3.4. Compound 20 induced apoptosis via up-regulating Noxa

To further check if the apoptosis induced by compound **20** is though the intrinsic pathway, mitochondrial membrane potential (MMP/$\Delta\Psi$) were analyzed using flow cytometry. The loss of MMP in Kyse30 and Kyse450 were clearly observed as the concentration of compound **20** increases (Fig. 6A). These suggest that the compound **20** may induce cell apoptosis through intrinsic apoptosis pathway. Next, we determined the mitochondria apoptosis related proteins the Bcl-2 family and XIAP. As shown in Fig. 6B, in both cell lines, pro-apoptosis proteins Bid, Bim, Noxa were up regulated, the anti-apoptosis protein Bcl-2, Mcl-1, XIAP were down regulated, while the Bax, Bak do not have significant changes. Among which Noxa made the most tremendous changes after the treatment in both cell lines. Next siRNA silencing was performed to downregulate Noxa. In the Noxa silenced cell lines, the apoptosis and PARP cleavage induced by compound **20** had been evidently rescued (Fig. 6C and D). In conclusion, the apoptosis induced by compound **20** is via intrinsic apoptosis pathway and depend on the participation of Noxa.

3. Conclusions

A series of novel indoline derivatives were design, synthesized and evaluated for their antiproliferative activity. Kyse30 was chosen to determine the anti-cancer mechanisms, three other cancer cell lines were used to appraise the broad-spectrum anti-cancer activity. Compound **20** inhibits tumor growth against ESCC cell lines *in vitro* and *in vivo*. Mechanism studies showed that compound **20** could arrest the cells at M phase. In addition, compound **20** induced Noxa-dependent apoptosis. These observations demonstrate that indoline **20** might be a lead compound for the discovery of more Noxa mediated apoptosis inducers against esophageal squamous cell carcinoma.
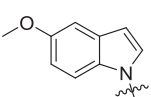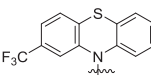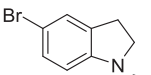
4. Experimental section
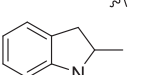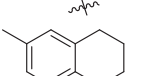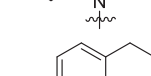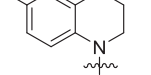
4.1. General chemistry

All chemical agents were obtained from Bei Jing Yinuo Kai company. Melting points were taken on an X-5 micromelting apparatus from Shang Hai Jing Ke company. ^{1}H and ^{13}C NMR spectra were respectively determined with a 400 and 100 MHz spectrometer (Agilent, Santa Clara, CA, USA). Mass spectra w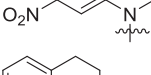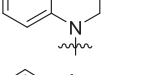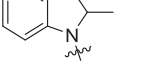ere recorded on Esquire 3000 mass spectrometer (Varian, Palo Alto, CA, USA). The spectra data of compounds are provided in the supporting information.

4.2. General procedure for the synthesis of compounds 12–13

To a solution of 5-(bromomethyl)-1,2,3-trimethoxybenzene **11** (6 mmol) in acetone (30 ml), K$_2$CO$_3$ (7 mmol) and arylamine (6 mmol) were added. After the mixture was stirred at 60 °C for 5 h. The organic layer was concentrated and then purified by column chromatography with petroleum/ethyl acetate (9:1) to afford the target compound **12–13**.

Table 2
Antiproliferative activity of the synthetic derivatives **18–27**.

Compound	N-heterocycle	R$_1$	IC$_{50}$ (µM)[a]			
			Hela	A549	HepG2	KYSE30
5FU	–	–	22.08 ± 0.05	4.22 ± 0.04	1.32 ± 0.04	1.46 ± 0.03
18		3,4,5-trimethoxy	4.66 ± 0.02	2.74 ± 0.05	1.35 ± 0.06	1.54 ± 0.05
19		3,4,5-trimethoxy	6.36 ± 0.04	18.06 ± 0.05	16.14 ± 0.13	19.45 ± 0.08
20		3,4,5-trimethoxy	1.30 ± 0.08	1.24 ± 0.05	1.42 ± 0.05	1.21 ± 0.06
21		3,4,5-trimethoxy	3.24 ± 0.04	4.30 ± 0.04	27.97 ± 0.07	38.04 ± 0.15
22		3,4,5-trimethoxy	2.32 ± 0.09	4.00 ± 0.05	1.92 ± 0.03	1.31 ± 0.09
23		3,4,5-trimethoxy	4.60 ± 0.04	4.05 ± 0.05	12.29 ± 0.04	6.53 ± 0.06
24		3,4-dimethoxy	> 80	> 80	14.56 ± 0.03	5.72 ± 0.05
25		3,4-dimethoxy	7.08 ± 0.05	> 80	13.55 ± 0.04	14.51 ± 0.05
26		3,4-dimethoxy	7.73 ± 0.05	> 80	24.93 ± 0.06	6.79 ± 0.05
27		4-methoxy	5.83 ± 0.07	> 80	12.96 ± 0.06	7.37 ± 0.15

[a] Antiproliferative activity was assayed by exposure for 48 h. Data are presented as the means ± SDs from the dose-response curves of three independent experiments.

4.3. General procedure for the synthesis of compounds 15–27 and 29–32

Formyl chloride derivatives (7 mmol) was added to the solution of various arylamines (7 mmol) in acetone (25 ml). After stirring at 60 °C for 6 h, the reaction mixture was concentrated to remove acetone. The residue was purified by column chromatography with petroleum/ethyl acetate (9:1) to afford the target compound **15–27** and **29–32**.

#### 4.3.1. 1-(3,4,5-Trimethoxybenzyl)-1,2,3,4-tetrahydroquinoline (12)

White solid, m.p.: 62–63 °C, yield: 80%. ^{1}H NMR (400 MHz, CDCl$_3$) δ 7.04–6.93 (m, 2H), 6.65–6.52 (m, 2H), 6.50 (s, 2H), 4.39 (s, 2H), 3.82 (d, J = 10.5 Hz, 9H), 3.41–3.26 (m, 2H), 2.82 (t, J = 6.3 Hz, 2H), 2.01

(dt, J = 11.8, 6.1 Hz, 2H). ^{13}C NMR (100 MHz, CDCl$_3$) δ 153.50, 145.80, 136.73, 134.86, 129.04, 127.17, 122.47, 116.14, 111.30, 103.31, 60.86, 56.10, 55.67, 49.83, 28.20, 22.46. HRMS (ESI): Calcd. C$_{19}$H$_{24}$NO$_3$, [M + H]$^+$ m/z: 314.1756, found: 314.1759.

4.3.2. 1-(3,4,5-Trimethoxybenzyl)indoline (13)

White solid, m.p.: 71–72 °C, yield: 75%. ^{1}H NMR (400 MHz, CDCl$_3$) δ 7.15–7.02 (m, 2H), 6.69 (t, J = 7.3 Hz, 1H), 6.60 (s, 2H), 6.53 (d, J = 7.8 Hz, 1H), 4.17 (s, 2H), 3.84 (d, J = 4.2 Hz, 9H), 3.31 (t, J = 8.3 Hz, 2H), 2.98 (t, J = 8.3 Hz, 2H). ^{13}C NMR (100 MHz, CDCl$_3$) δ 152.31, 151.51, 135.93, 133.24, 129.09, 126.29, 123.53, 117.00, 106.31, 103.57, 59.84, 55.10, 53.32, 52.80, 27.53. HRMS (ESI): Calcd.

Table 3
Antiproliferative activity of the synthetic derivatives **29–32**.
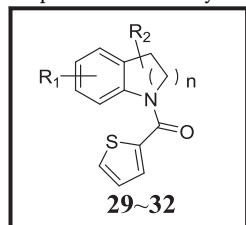
Compound		IC$_{50}$ (μM)[a]			
		Hela	A549	HepG2	KYSE30
5FU	–	22.08 ± 0.05	4.22 ± 0.04	1.32 ± 0.04	1.46 ± 0.03
29		3.87 ± 0.12	7.32 ± 0.04	20.85 ± 0.08	8.56 ± 0.08
30		9.11 ± 0.04	6.65 ± 0.04	7.34 ± 0.07	24.61 ± 0.13
31		> 80	> 80	2.12 ± 0.04	7.86 ± 0.10
32		> 80	11.05 ± 0.06	5.75 ± 0.03	30.97 ± 0.10

[a] Antiproliferative activity was assayed by exposure for 48 h. Data are presented as the means ± SDs from the dose-response curves of three independent experiments.

C$_{18}$H$_{22}$NO$_3$, [M + H]$^+$ *m/z*: 300.1600, found: 300.1607.

4.3.3. (3,4-Dihydroquinolin-1(2H)-yl)(3,4,5-trimethoxyphenyl) methanone (15)

White solid, m.p.: 102–103 °C, yield: 60%. ^{1}H NMR (400 MHz, CDCl$_3$) δ 7.06 (d, *J* = 7.3 Hz, 1H), 6.91 (t, *J* = 7.3 Hz, 1H), 6.82 (t, *J* = 7.5 Hz, 1H), 6.66 (d, *J* = 7.8 Hz, 1H), 6.50 (s, 2H), 3.82 (t, *J* = 6.5 Hz, 2H), 3.74 (s, 3H), 3.58 (s, 6H), 2.75 (t, *J* = 6.5 Hz, 2H), 2.06–1.85 (m, 2H). ^{13}C NMR (100 MHz, CDCl$_3$) δ 168.60, 151.69, 138.80, 138.51, 130.65, 129.96, 127.16, 124.85, 124.34, 123.59, 105.48, 59.84, 55.01, 43.53, 25.94, 23.22. HRMS (ESI): Calcd. C$_{19}$H$_{22}$NO$_4$, [M + H]$^+$ *m/z*: 328.1549, found: 328.1552.

4.3.4. Indolin-1-yl(3,4,5-trimethoxyphenyl)methanone (16)

White solid, m.p.: 105–106 °C, yield: 90%. ^{1}H NMR (400 MHz, CDCl$_3$) δ 7.27 (s, 1H), 7.22 (d, *J* = 7.4 Hz, 1H), 7.12 (s, 1H), 7.02 (t, *J* = 7.1 Hz, 1H), 6.78 (s, 2H), 4.12 (t, *J* = 8.0 Hz, 2H), 3.88 (d, *J* = 14.8 Hz, 9H), 3.13 (t, *J* = 8.3 Hz, 2H). ^{13}C NMR (100 MHz, CDCl$_3$) δ 168.58, 153.38, 142.51, 139.78, 132.42, 132.20, 127.24, 124.96, 123.95, 123.89, 104.55, 60.98, 56.29, 50.45, 28.06. HRMS (ESI): Calcd. C$_{18}$H$_{20}$NO$_4$, [M + H]$^+$ *m/z*: 314.1392, found: 314.1398.

4.3.5. (2,3,4,5-tetrahydro-1H-benzo[b]azepin-1-yl)(3,4,5-trimethoxyphenyl)methanone (17)

White solid, m.p.: 144–145 °C, yield: 50%. ^{1}H NMR (400 MHz, CDCl$_3$) δ 7.16 (d, *J* = 7.5 Hz, 1H), 7.02 (t, *J* = 7.4 Hz, 1H), 6.89 (t, *J* = 7.5 Hz, 1H), 6.60 (d, *J* = 7.7 Hz, 1H), 6.38 (s, 2H), 4.95 (d, *J* = 13.2 Hz, 1H), 3.69 (s, 3H), 3.52 (s, 6H), 2.97 (t, *J* = 13.0 Hz, 1H), 2.82 (dd, *J* = 13.6, 4.4 Hz, 1H), 2.71 (t, *J* = 10.1 Hz, 1H), 2.02 (d, *J* = 11.5 Hz, 1H), 1.89 (dd, *J* = 11.8, 7.5 Hz, 2H), 1.45 (d, *J* = 11.5 Hz, 1H). ^{13}C NMR (100 MHz, CDCl$_3$) δ 167.16, 151.25, 143.46, 138.14, 138.01, 129.72, 128.78, 127.15, 126.31, 126.20, 105.23, 59.78, 54.85,

46.75, 33.85, 28.65, 25.27. HRMS (ESI): Calcd. C$_{20}$H$_{24}$NO$_4$, [M + H]$^+$ *m/z*: 342.1705, found: 342.1709.

4.3.6. (5-Methoxy-1H-indol-1-yl)(3,4,5-trimethoxyphenyl)methanone (18)

Yellow liquid, yield: 65%. ^{1}H NMR (400 MHz, CDCl$_3$) δ 8.18 (d, *J* = 9.0 Hz, 1H), 7.26 (d, *J* = 3.7 Hz, 1H), 6.98 (d, *J* = 2.5 Hz, 1H), 6.91 (dd, *J* = 9.1, 2.5 Hz, 1H), 6.89 (s, 2H), 6.47 (d, *J* = 3.7 Hz, 1H), 3.86 (s, 3H), 3.81 (s, 6H), 3.79 (s, 3H). ^{13}C NMR (100 MHz, CDCl$_3$) δ 166.84, 155.71, 152.17, 140.21, 130.74, 129.74, 128.52, 127.18, 116.09, 112.38, 107.43, 105.79, 102.59, 59.98, 55.36, 54.67. HRMS (ESI): Calcd. C$_{19}$H$_{20}$NO$_5$, [M + H]$^+$ *m/z*: 342.1341, found: 342.1347.

### 4.3.7. (2-(Trifluoromethyl)-10H-phenothiazin-10-yl)(3,4,5-trimethoxyphenyl)methanone (19)

White solid, m.p.: 159–160 °C, yield: 43%. ^{1}H NMR (400 MHz, DMSO) δ 7.91 (s, 1H), 7.83 (d, *J* = 8.2 Hz, 1H), 7.72–7.55 (m, 2H), 7.38 (dd, *J* = 6.4, 2.7 Hz, 1H), 7.35–7.21 (m, 2H), 6.60 (s, 2H), 3.63 (s, 3H), 3.59 (s, 6H). ^{13}C NMR (100 MHz, DMSO) δ 167.34, 152.30, 139.36, 138.98, 138.53, 136.90, 130.19, 129.11, 128.51, 127.76, 127.66, 127.36, 127.12, 127.05, 125.05, 123.54, 123.23, 122.34, 106.25, 60.07, 55.78. HRMS (ESI): Calcd. C$_{23}$H$_{19}$F$_3$NO$_4$S, [M + H]$^+$ *m/z*: 462.0987, found: 462.0989.

4.3.8. (5-Bromoindolin-1-yl)(3,4,5-trimethoxyphenyl)methanone (20)

White solid, m.p.: 126–127 °C, yield: 31%. ^{1}H NMR (400 MHz, DMSO) δ 7.89 (s, 1H), 7.48 (s, 1H), 7.37 (d, *J* = 7.9 Hz, 1H), 6.90 (s, 2H), 4.06 (t, *J* = 8.4 Hz, 2H), 3.82 (d, *J* = 8.0 Hz, 6H), 3.73 (d, *J* = 4.9 Hz, 3H), 3.10 (t, *J* = 8.3 Hz, 2H). ^{13}C NMR (100 MHz, DMSO) δ 168.29, 153.28, 142.63, 139.31, 136.21, 132.46, 130.03, 128.30, 115.66, 107.00, 105.02, 60.57, 56.58. HRMS (ESI): Calcd. C$_{18}$H$_{19}$BrNO$_4$, [M + H]$^+$ *m/z*: 392.0497, found: 392.0499.
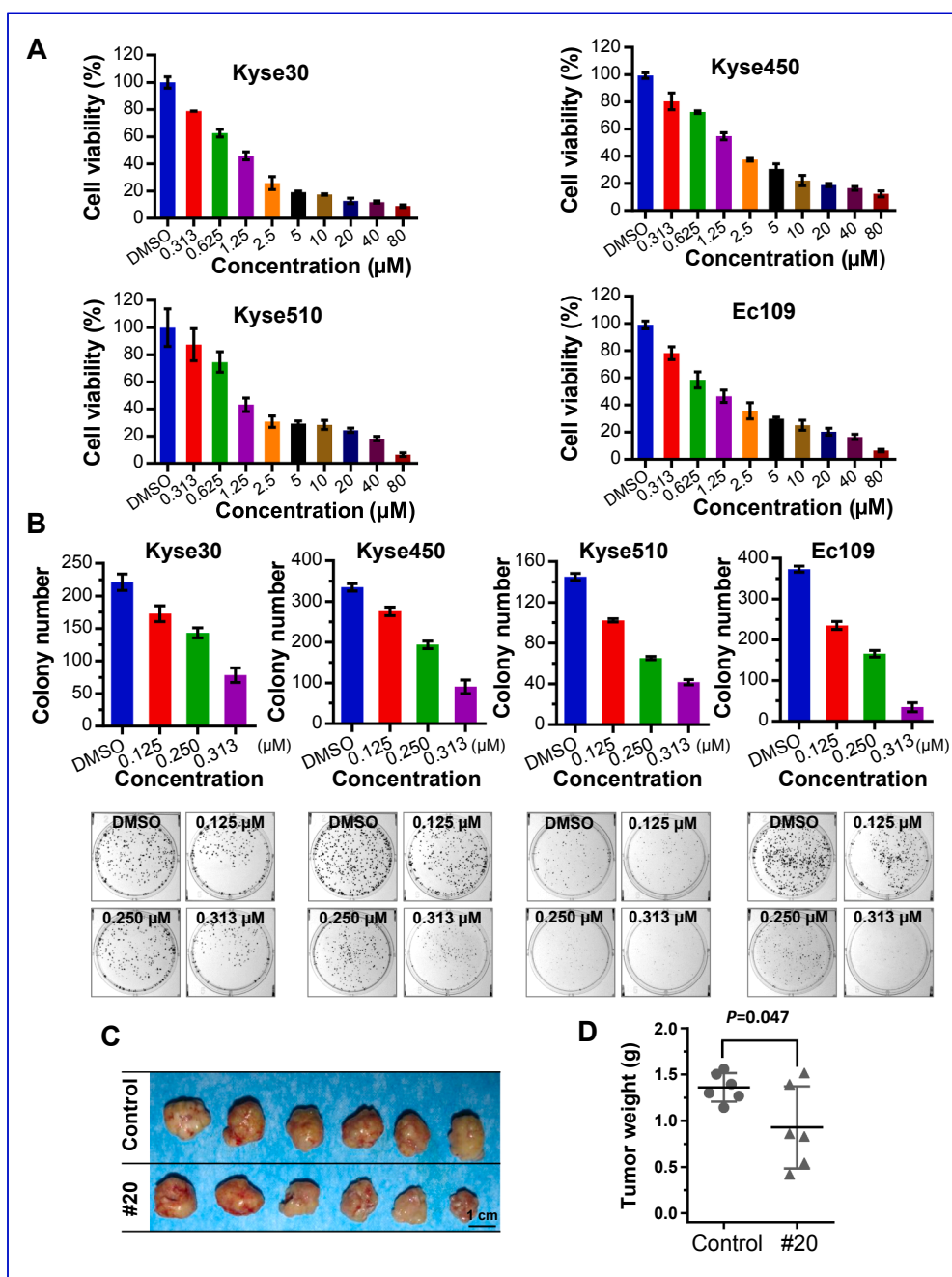
Fig. 3. A. Cell viabilities of four ESCC cell lines after 48 h compound **20** treatment; **B**. 4 ESCC cell lines colonies formed after 7 days compound **20** treatment; **C&D**. Tumors and tumors' weight after 30 days compound **20** treatment.

4.3.9. (2-Methylindolin-1-yl)(3,4,5-trimethoxyphenyl)methanone (21)

White solid, m.p.: 102–103 °C, yield: 23%. ^{1}H NMR (400 MHz, CDCl$_3$) δ 7.13 (d, J = 7.1 Hz, 1H), 6.92 (dt, J = 15.5, 7.7 Hz, 3H), 6.66 (s, 2H), 4.77–4.63 (m, 1H), 3.81 (s, 3H), 3.75 (s, 6H), 3.34 (dd, J = 15.7, 8.8 Hz, 1H), 2.56 (dd, J = 15.7, 1.1 Hz, 1H), 1.21 (d, J = 6.3 Hz, 3H). ^{13}C NMR (100 MHz, CDCl$_3$) δ 168.31, 153.39, 141.29, 139.71, 132.18, 131.51, 127.01, 125.48, 123.78, 116.78, 104.67, 60.96, 57.13, 56.28, 35.84, 20.84. HRMS (ESI): Calcd. C$_{19}$H$_{22}$NO$_4$, [M +H]$^+$ m/z: 328.1549, found: 328.1554.

4.3.10. (6-Methyl-3,4-dihydroquinolin-1(2H)-yl)(3,4,5-trimethoxyphenyl)methanone (22)

White solid, m.p.: 92–93 °C, yield: 37%. ^{1}H NMR (400 MHz, DMSO) δ 7.01 (s, 1H), 6.77 (s, 2H), 6.62 (s, 2H), 3.71 (t, J = 6.4 Hz, 2H), 3.67

(s, 3H), 3.64 (s, 6H), 2.77 (t, J = 6.6 Hz, 2H), 2.21 (s, 3H), 1.92 (p, J = 6.5 Hz, 2H). ^{13}C NMR (100 MHz, CDCl$_3$) δ 168.53, 151.66, 138.62, 135.89, 133.24, 130.38, 130.17, 127.61, 125.58, 124.11, 105.35, 59.89, 55.00, 43.56, 25.88, 23.24, 19.77. HRMS (ESI): Calcd. C$_{20}$H$_{24}$NO$_4$, [M + H]$^+$ m/z: 342.1705, found: 342.1708.

4.3.11. (7-Nitro-3,4-dihydroquinolin-1(2H)-yl)(3,4,5-trimethoxyphenyl) methanone (23)

White solid, m.p.: 129–130 °C, yield: 21%. ^{1}H NMR (400 MHz, DMSO) δ 8.21 (s, 1H), 7.94 (dd, J = 8.4, 2.4 Hz, 1H), 7.54 (d, J = 8.5 Hz, 1H), 6.85 (s, 2H), 3.83–3.80 (m, 2H), 3.79 (d, J = 5.1 Hz, 6H), 3.74 (s, 3H), 3.01 (t, J = 6.6 Hz, 2H), 2.09–1.93 (m, 2H). ^{13}C NMR (100 MHz, DMSO) δ 170.24, 153.24, 145.51, 139.65, 139.61, 138.86, 131.47, 130.50, 119.52, 118.71, 105.97, 60.60, 56.55, 46.44, 27.15,

7
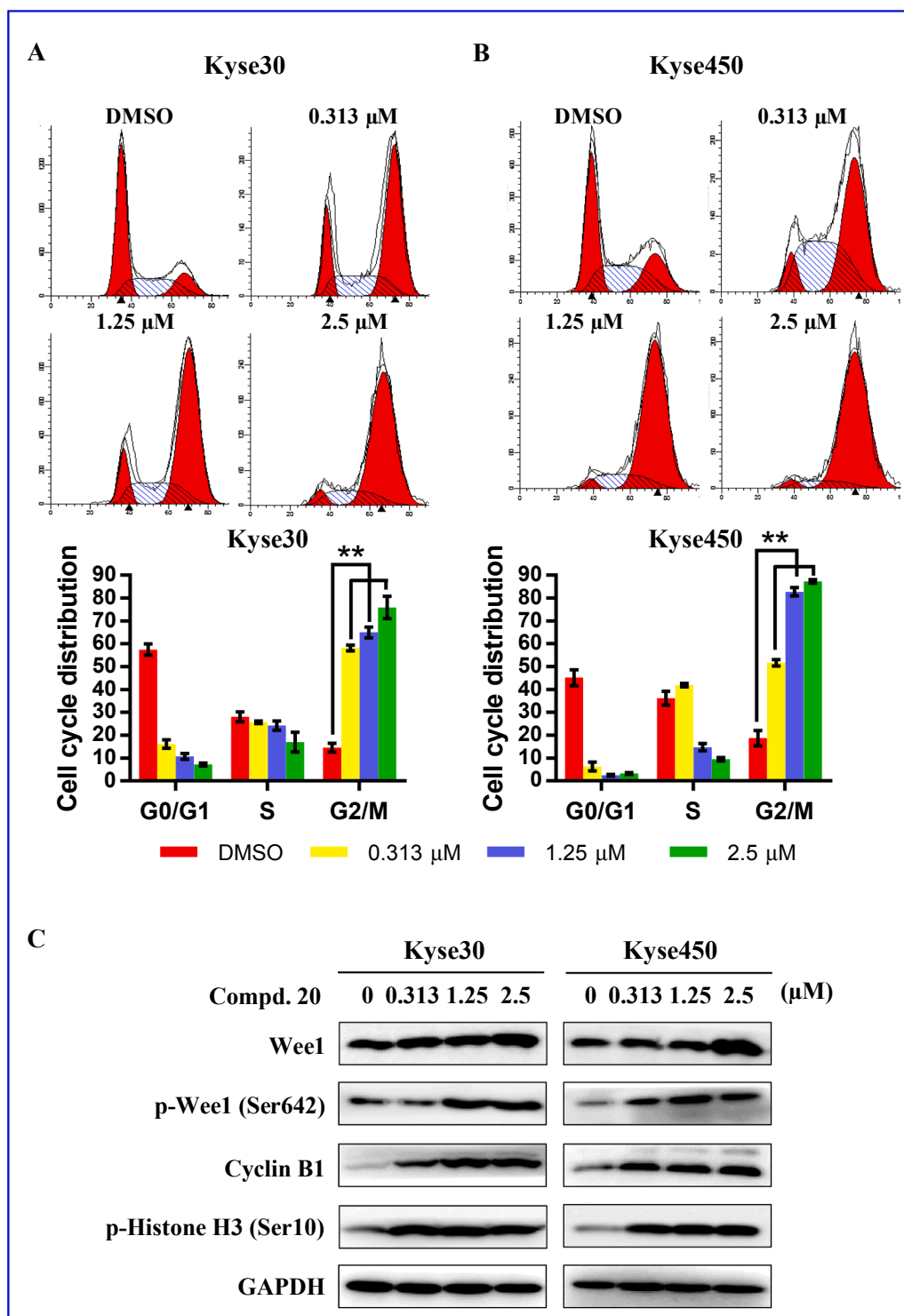
Fig. 4. A&B. Two cell lines were treated with compound **20** as shown in this figure for 48 h, and cell cycle phases' percentage were analyzed; **C**. The change of cell cycle related proteins in cells after 48 h treatment by compound **20**.

22.97. HRMS (ESI): Calcd. $C_{19}H_{21}N_2O_6$, $[M+H]^+$ *m/z*: 373.1400, found: 373.1406.

### 4.3.12. (3,4-Dihydroquinolin-1(2H)-yl)(3,4-dimethoxyphenyl)methanone (24)

White solid, m.p.: 117–118 °C, yield: 30%. ^{1}H NMR (400 MHz, CDCl$_3$) δ 7.08 (d, $J = 7.4$ Hz, 1H), 6.92 (t, $J = 7.4$ Hz, 1H), 6.88–6.84 (m, 2H), 6.81 (t, $J = 7.7$ Hz, 1H), 6.63 (dd, $J = 8.3, 4.9$ Hz, 2H), 3.84 (t, $J = 6.6$ Hz, 2H), 3.79 (s, 3H), 3.65 (s, 3H), 2.76 (t, $J = 6.6$ Hz, 2H),

1.99 (p, $J = 6.6$ Hz, 2H). ^{13}C NMR (100 MHz, CDCl$_3$) δ 168.84, 149.64, 147.30, 138.84, 130.63, 127.24, 127.18, 124.80, 124.42, 123.36, 121.45, 111.19, 109.03, 54.85, 54.75, 43.40, 25.98, 23.25. HRMS (ESI): Calcd. $C_{18}H_{20}NO_3$, $[M+H]^+$ *m/z*: 298.1443, found: 298.1447.

4.3.13. (3,4-Dimethoxyphenyl)(2-methylindolin-1-yl)methanone (25)

White solid, m.p.: 130–131 °C, yield: 27%. ^{1}H NMR (400 MHz, CDCl$_3$) δ 7.13 (d, $J = 7.0$ Hz, 1H), 7.08–6.93 (m, 3H), 6.91 (dd, $J = 16.4, 9.1$ Hz, 2H), 6.80 (d, $J = 8.2$ Hz, 1H), 4.87–4.59 (m, 1H), 3.86
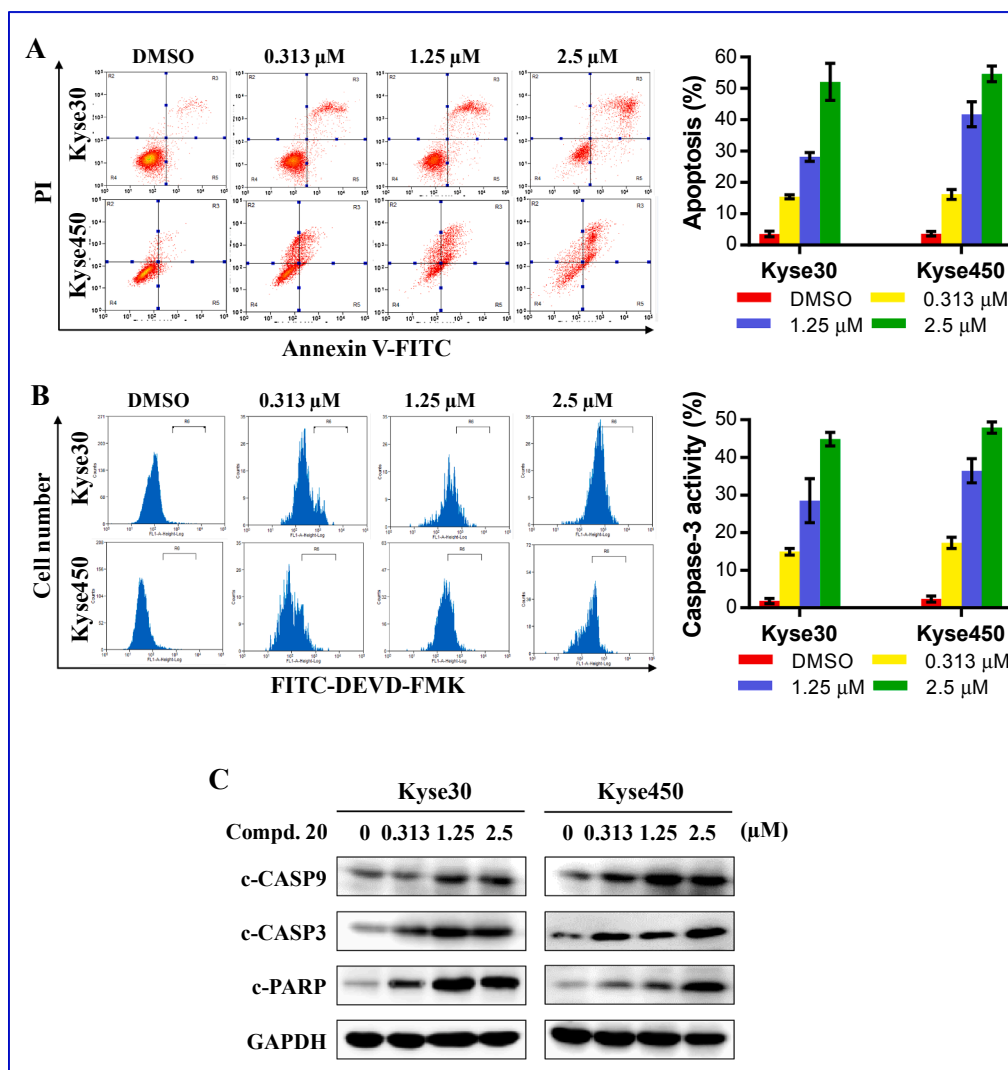
Fig. 5. A. The activity of compound **20** to induce apoptosis after 72 h treatment; Representative images were shown (left panel). The early apoptotic (Annexin V-FITC positive) and late apoptotic (Annexin V-FITC positive, PI positive) were quantified as apoptotic cells. The percentage of apoptotic cells were shown in right panel. **B**. The activity of compound **20** to activate Caspase-3 after 72 h treatment; Representative images were shown (left panel). The percentage of cells with active caspase 3 was shown in right panel. **C**. The change of cleaved-Caspase 9, cleaved-Caspase-3, cleaved PARP in cells after 72 h treatment by compound **20**.

(s, 3H), 3.80 (s, 3H), 3.34 (dd, $J = 15.3$, 8.9 Hz, 1H), 2.57 (dd, $J = 15.7$, 1.4 Hz, 1H), 1.21 (d, $J = 6.3$ Hz, 3H). ^{13}C NMR (100 MHz, CDCl$_3$) δ 167.54, 149.71, 147.93, 140.65, 130.52, 128.27, 125.92, 124.44, 122.50, 119.56, 115.70, 109.82, 109.58, 56.27, 55.01, 54.96, 34.87, 19.68. HRMS (ESI): Calcd. C$_{18}$H$_{20}$NO$_3$, [M+H]$^+$ m/z: 298.1443, found: 298.1446.

4.3.14. (3,4-Dimethoxyphenyl)(6-methyl-3,4-dihydroquinolin-1(2H)-yl)methanone (26)

White solid, m.p.: 109–110 °C, yield: 43%. ^{1}H NMR (400 MHz, CDCl$_3$) δ 6.95–6.80 (m, 3H), 6.68–6.57 (m, 2H), 6.50 (d, $J = 8.2$ Hz, 1H), 3.82 (t, $J = 6.6$ Hz, 2H), 3.79 (s, 3H), 3.66 (s, 3H), 2.72 (t, $J = 6.6$ Hz, 2H), 2.18 (s, 3H), 1.96 (p, $J = 6.6$ Hz, 2H). ^{13}C NMR (100 MHz, CDCl$_3$) δ 169.73, 150.56, 148.31, 137.28, 133.99, 131.38, 128.69, 128.47, 126.55, 125.19, 122.38, 112.22, 110.05, 55.87, 55.78, 44.43, 26.93, 24.29, 20.81. HRMS (ESI): Calcd. C$_{19}$H$_{22}$NO$_3$, [M+H]$^+$ m/z: 312.1600, found: 312.1605.

4.3.15. (3,4-Dihydroquinolin-1(2H)-yl)(4-methoxyphenyl)methanone (27)

White solid, m.p.: 84–85 °C, yield: 54%. ^{1}H NMR (400 MHz, CDCl$_3$) δ 7.25 (d, $J = 8.8$ Hz, 2H), 7.07 (d, $J = 7.2$ Hz, 1H), 6.95–6.86 (m, 1H),

6.81 (dd, $J = 11.2$, 4.2 Hz, 1H), 6.73–6.65 (m, 2H), 6.62 (d, $J = 8.0$ Hz, 1H), 3.82 (dd, $J = 8.0$, 5.2 Hz, 2H), 3.71 (s, 3H), 2.76 (t, $J = 6.6$ Hz, 2H), 1.97 (p, $J = 6.6$ Hz, 2H). ^{13}C NMR (100 MHz, CDCl$_3$) δ 168.94, 160.06, 138.80, 130.52, 129.75, 127.30, 127.27, 124.73, 124.39, 123.28, 112.24, 54.24, 43.38, 25.96, 23.21. HRMS (ESI): Calcd. C$_{17}$H$_{18}$NO$_2$, [M+H]$^+$ m/z: 268.1338, found: 268.1339.

4.3.16. (2-Methylindolin-1-yl)(thiophen-2-yl)methanone (29)

Yellow liquid, yield: 72%. ^{1}H NMR (400 MHz, DMSO) δ 8.00–7.72 (m, 2H), 7.71 (d, $J = 3.7$ Hz, 1H), 7.32 (d, $J = 7.3$ Hz, 1H), 7.25–7.13 (m, 2H), 7.08 (t, $J = 7.4$ Hz, 1H), 5.15–4.91 (m, 1H), 3.48 (d, $J = 8.7$ Hz, 1H), 2.71 (d, $J = 15.9$ Hz, 1H), 1.19 (d, $J = 6.4$ Hz, 3H). ^{13}C NMR (100 MHz, DMSO) δ 161.31, 142.18, 139.22, 131.80, 131.16, 129.89, 128.25, 127.46, 125.90, 124.64, 117.71, 57.05, 36.37, 21.73. HRMS (ESI): Calcd. C$_{14}$H$_{13}$NOS, [M+H]$^+$ m/z: 243.0718, found: 243.0719.

4.3.17. (5-Bromoindolin-1-yl)(thiophen-2-yl)methanone (30)

White solid, m.p.: 118–119 °C, yield: 32%. ^{1}H NMR (400 MHz, DMSO) δ 7.97 (d, $J = 8.5$ Hz, 1H), 7.88 (dd, $J = 5.0$, 0.9 Hz, 1H), 7.81–7.65 (m, 1H), 7.49 (s, 1H), 7.38 (d, $J = 8.6$ Hz, 1H), 7.22 (dd, $J = 5.0$, 3.8 Hz, 1H), 4.43 (t, $J = 8.4$ Hz, 2H), 3.21 (t, $J = 8.3$ Hz, 2H).
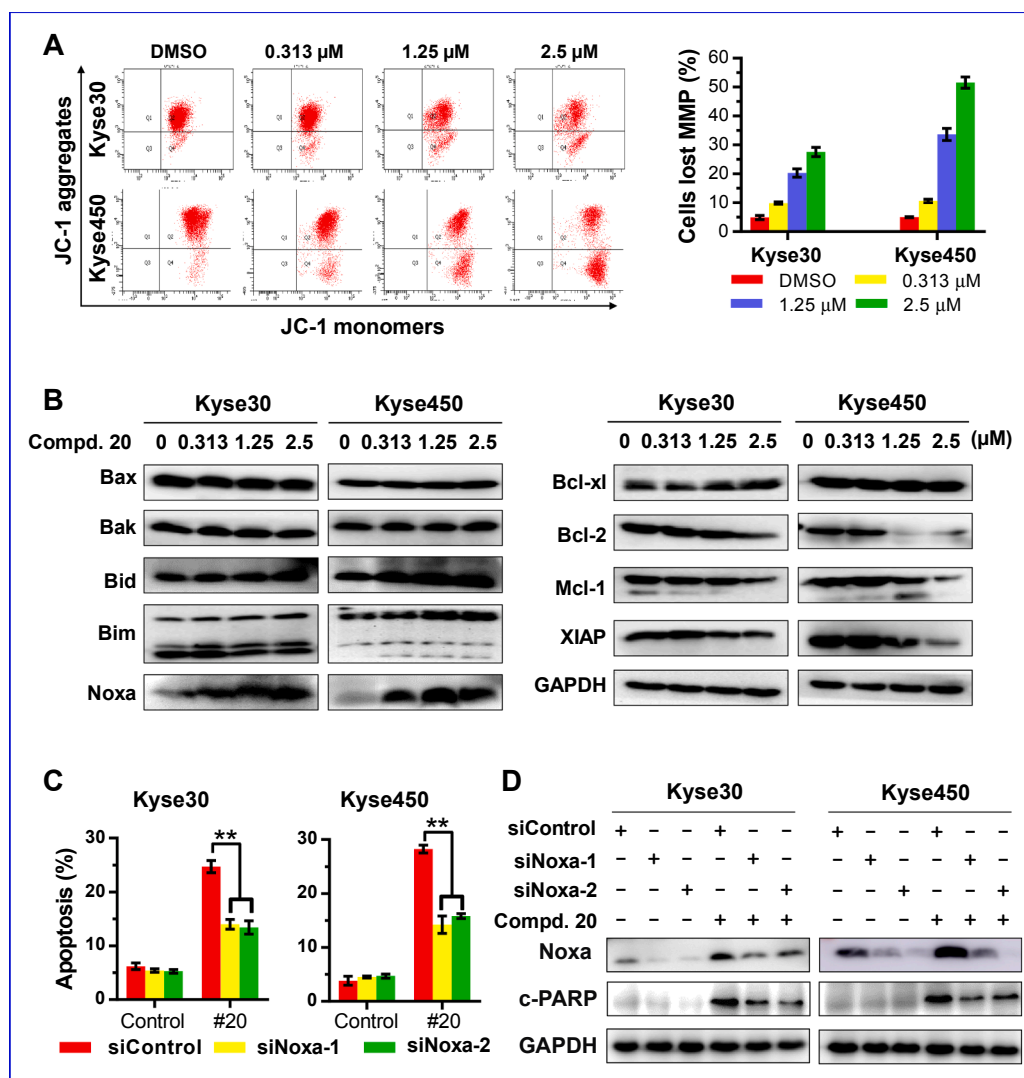
Fig. 6. A. Mitochondrial membrane potential change of both cells after 24 h compound **20** treatment; Representative images were shown in left panel; Percentage of cells that had lost mitochondrial membrane potential is shown in right panel. **B.** The change of mitochondrial related proteins in cells after 72 h treatment by compound **20**; **C &D.** Downregulation of Noxa reduced compound **20**-induced apoptosis. Kyse30 and Kyse450 cells were transfected with control siRNA or Noxa siRNA and then treated with DMSO or 1.25 μmol/L compound **20** for 48 h. Apoptosis induction was quantified by Annexin V-FITC/PI double-staining analysis. Knockdown efficiency and cleaved PARP were assessed by western blot assay.

^{13}C NMR (100 MHz, DMSO) δ 161.21, 142.99, 139.62, 135.92, 132.07, 130.92, 130.11, 128.42, 128.22, 118.99, 115.93, 50.80, 28.40. HRMS (ESI): Calcd. $C_{13}H_{11}BrNOS$, $[M+H]^+$ m/z: 307.9745, found: 307.9748.

4.3.18. Indolin-1-yl(thiophen-2-yl)methanone (31)

White solid, m.p.: 95–96 °C, yield: 14%. ^{1}H NMR (400 MHz, DMSO) δ 8.03 (d, $J = 7.8$ Hz, 1H), 7.87 (d, $J = 5.0$ Hz, 1H), 7.75 (d, $J = 3.7$ Hz, 1H), 7.29 (d, $J = 7.3$ Hz, 1H), 7.21 (dt, $J = 13.0, 6.3$ Hz, 2H), 7.06 (t, $J = 7.4$ Hz, 1H), 4.41 (t, $J = 8.3$ Hz, 2H), 3.20 (t, $J = 8.2$ Hz, 2H). ^{13}C NMR (100 MHz, CDCl$_3$) δ 160.48, 142.06, 138.43, 130.81, 129.10, 128.75, 126.46, 126.16, 123.64, 123.21, 116.74, 49.62, 27.66. HRMS (ESI): Calcd. $C_{13}H_{12}NOS$, $[M+H]^+$ m/z: 230.0640, found: 230.0647.

4.3.19. (3,4-Dihydroquinolin-1(2H)-yl)(thiophen-2-yl)methanone (32)

White solid, m.p.: 73–74 °C, yield: 55%. ^{1}H NMR (400 MHz, DMSO) δ 7.72 (dd, $J = 5.0, 1.1$ Hz, 1H), 7.24 (d, $J = 7.2$ Hz, 1H), 7.11–7.03 (m, 2H), 7.03–6.96 (m, 3H), 3.81 (t, $J = 6.5$ Hz, 2H), 2.77 (t, $J = 6.6$ Hz, 2H), 1.94 (p, $J = 6.6$ Hz, 2H). ^{13}C NMR (100 MHz, DMSO) δ 163.17, 139.39, 138.78, 132.69, 131.37, 131.09, 128.88, 127.49, 126.09, 125.52, 125.39, 45.22, 26.54, 24.30. HRMS (ESI): Calcd. $C_{14}H_{14}NOS$, $[M+H]^+$ m/z: 244.0796, found: 244.0798.

4.4. Cell culture

Hela, A549, HepG2, Kyse30, Kyse450, Kyse510, EC109 cell lines were cultured in an atmosphere with 5% CO_2 at 37 °C, using RPMI-1640 with 10% fetal bovine serum (FBS), 100 U/ml penicillin and 0.1 mg/ml streptomycin as culture medium.

4.5. CCK8 assay

Cells were seeded in 96-well plates at a density of 3×10^3 per well. After 24 h incubation, they were treated with different concentrations of compound as shown in the Figures and Tables. After 48 h, 5 μL CCK8 solution was added to each well, and co-incubated for 4 h at 37 °C. The absorbance was determined at 450 nm. Data are calculated with GraphPad Prism5 software.

4.6. Colony formation assay

Kyse30, Kyse450, Kyse510 and EC109 cells were seeded in a 6-well plate at a density of 5×10^2 per well and incubated at 37 °C in 5% CO_2 for 24 h, then they were treated with different concentrations of compound 20. After 7 days, the culture medium was removed, and the cells were washed with PBS and fix with 4% paraformaldehyde. Then stain the cells with 0.1% crystal violet. The images were captured with camera. Colonies comprising 50 cells or more were counted.

4.7. Cell cycle distribution assay

Kyse30 and Kyse450 cells were seeded in 6-well culture plate. After 24 h incubation, cells were treated with certain concentration of compound 20 for 24 h. Then cells were harvested and fixed at 4 °C with 70% ethanol. The fixed cells were washed twice and resuspended using PBS with 10 mg/mL RNaseA and 50 mg/mL PI incubated for 30 min in the dark. Samples were analyzed for DNA content with flow cytometry then (Becton, Dickinson and Company, NJ). Data were analyzed with ModFit LT software (Verity).

4.8. Cell apoptosis assay

Kyse30 and Kyse450 cells were seeded in 6-well culture plate and treated with certain concentration of compound 20 as shown in Figures for 72 h. Cells were harvested and suspended in binding buffer containing Annexin V-FITC (0.5 mg/mL) and PI (0.5 mg/mL) then. After that, samples were incubated for 25 min in dark and analyzed with flow cytometry (Becton, Dickinson and Company, NJ). The activities of caspase-3 were quantitated by CaspGLOW Fluorescein Active Caspase-3 Staining Kit (BioVision, Inc. Milpitas, California) according to the manufacturer's instructions.

4.9. Activity assays of caspase-3

1.5×10^5 (Kyse30) or 1×10^5 (Kyse450) cells were seeded per well in 6-well plates. After 24 h, the cells were maintained with the indicated concentration of compound 20 for 72 h. The cells were collected and washed by PBS, and then resuspended with wash buffer supplied with the kit (Bio Vision, Inc. Milpitas, California).1 μL of FITC-DEVD-FMK was added into tubes above-mentioned. And the cells were incubated for 1 h at 37°C. Then cells were centrifuged at 3000 rpm for 5 min and washed. Finally, the cells were resuspended in 0.5 ml of wash buffer on ice, then analyzed by flow cytometry (Becton Dickinson FACScan; Becton-Dickinson, San Jose, CA, USA).

4.10. Western blot analysis

Treated and untreated cells were harvested and lysed. Cell extracts were denatured by loading buffer and resolved by SDS-PAGE and transferred to PVDF membrane. The membranes were incubated with appropriate primary antibodies at 4 °C for 10 h after blocking with 5% skimmed milk. After conjugated with secondary antibodies, the detection of proteins was carried out with an ECL kit.

4.11. Measurement of mitochondrial membrane potential (MMP, ΔΨ)

JC-1 probe was used as a measure of loss of MMP. Cells were seeded at 1.5×10^5 into 6-well plates and treated with certain concentrations of compound 20 for 24 h. Then JC-1 (2.5 μg/ml), were added and co-incubate with an equal volume of cell suspension at 37 °C for 15 min. Then, cells were washed with PBS. Then samples were analyzed with flow cytometry (Becton, Dickinson and Company, NJ).

4.12. Gene silencing using small interfering RNA (siRNA)

Kyse30 and Kyse450 cells were seeded at a density of 5×10^5 cells into 60-mm dishes and transfected with siRNA oligonucleotides (final concentration: 100 nmol/L), synthesized by GenePharma (Shanghai, China) using Lipofectamine 2000 (Cat. No. 11668019, Thermo Fisher Scientific). Cells were transfected with siRNA for 48 h and further treated with 1.25 μmol/L compound 20 for 48 h. The sequences of the siRNA are as follows: siNOXA-1: GUAAUUAUUGACACAUUUC; siNOXA-2: GGUGCACGUUUCAUCAAUUUG; siControl: UUCUCCG AACGUGUCACGU.

4.13. Subcutaneous transplantation tumor model of human esophageal cancer and treatment

A subcutaneous transplantation tumor model of human esophageal cancer was established using Kyse450 esophageal cancer cells. The tumor-bearing mice were randomized into 2 groups and subcutaneous injection with normal saline or compound 20 (150 mg/kg) continuously for 30 days (compound 20 was firstly resolved with the mixture of ethyl alcohol and castor oil, and then diluted in normal saline). Tumor size was determined by caliper measurement. The tumor volume was calculated using the ellipsoid volume formula (Length × Width^2/2). Tumor tissues were harvested, photographed, and weighed. Animal experiments were performed in accordance with animal protocols approved by the Institutional Animal Care and Use Committee of Zhengzhou University.

4.14. Statistical analysis

Data from three independent experiments are presented as mean ± SD. IC50 values and Student's t-tests were calculated by GraphPad Prism5 software. ** Respectively represent $p < 0.01$.

4.15. Abbreviations

Structure-activity relationships	SARs
Esophageal squamous cell carcinoma	ESCC
Histone deacetylase 6	HDAC6
Heat shock protein 90	HSP90
Human lung carcinoma cell line	A549
Human colon cancer cell line	HCT116
Human leukemia cell line	HL60
Human gastric carcinoma cell	MKN45
Human lung carcinoma cell line	H460
Human colon cancer cell line	HT29
Protein kinase R-like endoplasmic reticulum kinase	PERK
Human cervical cancer cell line	Hela
Human liver cancer cell line	HepG2
Human esophagus cancer cell line	KYSE30
5-Fluorouracil	5Fu
N, N′-ethylenebis (iodoacetamide)	EBI
Cyclin-dependent kinase 1	CDK1
Poly ADP-ribose polymerase	PARP
Mitochondrial membrane potential	MMP
B-cell lymphoma-2	Bcl-2
X-linked inhibitor of apoptosis protein	XIAP
Myeloid cell leukemia-1	MCl-1

Appendix A. Supplementary material

Supplementary data to this article can be found online at https://doi.org/10.1016/j.bioorg.2019.103190.

References

[1] T. Shiro, T. Fukaya, M. Tobe, The chemistry and biological activity of heterocycle-fused quinolinone derivatives: a review, Eur. J. Med. Chem. 97 (2015) 397–408.
[2] D.J. Fu, S.Y. Zhang, Y.C. Liu, L. Zhang, J.J. Liu, J. Song, R.H. Zhao, F. Li, H.H. Sun, H.M. Liu, Design, synthesis and antiproliferative activity studies of novel dithiocarbamate-chalcone derivates, Bioorg. Med. Chem. Lett. 26 (2016) 3918.
[3] D.-J. Fu, J.-J. Yang, P. Li, Y.-H. Hou, S.-N. Huang, M.A. Tippin, V. Pham, L. Song,

X. Zi, W.-L. Xue, L.-R. Zhang, S.-Y. Zhang, Bioactive heterocycles containing a 3,4,5-trimethoxyphenyl fragment exerting potent antiproliferative activity through microtubule destabilization, Eur. J. Med. Chem. 157 (2018) 50–61.

[4] D.J. Fu, L. Zhang, J. Song, R.W. Mao, R.H. Zhao, Y.C. Liu, Y.H. Hou, J.H. Li, J.J. Yang, C.Y. Jin, Design and synthesis of formononetin-dithiocarbamate hybrids that inhibit growth and migration of PC-3cells via MAPK/Wnt signaling pathways, Eur. J. Med. Chem. 127 (2016) 87–99.

[5] D.J. Fu, J. Song, Y.H. Hou, R.H. Zhao, J.H. Li, R.W. Mao, J.J. Yang, P. Li, X.L. Zi, Z.H. Li, Discovery of 5,6-diaryl-1,2,4-triazines hybrids as potential apoptosis inducers, Eur. J. Med. Chem. 138 (2017) 1076–1088.

[6] D.-J. Fu, S.-Y. Zhang, Y.-C. Liu, X.-X. Yue, J.-J. Liu, J. Song, R.-H. Zhao, F. Li, H.-H. Sun, Y.-B. Zhang, H.-M. Liu, Design, synthesis and antiproliferative activity studies of 1,2,3-triazole-chalcones, MedChemComm 7 (2016) 1664–1671.

[7] D.J. Fu, L. Fu, Y.C. Liu, J.W. Wang, Y.Q. Wang, B.K. Han, X.R. Li, C. Zhang, F. Li, J. Song, Structure-activity relationship studies of β2-lactam-azide analogues as orally active antitumor agents targeting the tubulin colchicine site, Sci. Rep. 7 (2017) 12788.

[8] S.C. Annedi, S.P. Maddaford, J. Ramnauth, P. Renton, T. Rybak, S. Silverman, S. Rakhit, G. Mladenova, P. Dove, J.S. Andrews, D. Zhang, F. Porreca, Discovery of a potent, orally bioavailable and highly selective human neuronal nitric oxide synthase (nNOS) inhibitor, N-(1-(piperidin-4-yl)indolin-5-yl)thiophene-2-carboximidamide as a pre-clinical development candidate for the treatment of migraine, Eur. J. Med. Chem. 55 (2012) 94–107.

[9] W.M. Eldehna, M. Fares, H.S. Ibrahim, M.H. Aly, S. Zada, M.M. Ali, S.M. Abou-Seri, H.A. Abdel-Aziz, D.A. Abou El Ella, Indoline ureas as potential anti-hepatocellular carcinoma agents targeting VEGFR-2: synthesis, in vitro biological evaluation and molecular docking, Eur. J. Med. Chem. 100 (2015) 89–97.

[10] Y. Lu, L. Wang, X. Wang, T. Xi, J. Liao, Z. Wang, F. Jiang, Design, combinatorial synthesis and biological evaluations of novel 3-amino-1′-((1-aryl-1H-1,2,3-triazol-5-yl)methyl)-2′-oxospiro[benzo[a] pyrano[2,3-c]phenazine-1,3′-indoline]-2-carbonitrile antitumor hybrid molecules, Eur. J. Med. Chem. 135 (2017) 125–141.

[11] R. Ojha, H.-L. Huang, W.-C. HuangFu, Y.-W. Wu, K. Nepali, M.-J. Lai, C.-J. Su, T.-Y. Sung, Y.-L. Chen, S.-L. Pan, J.-Y. Liou, 1-Aroylindoline-hydroxamic acids as anticancer agents, inhibitors of HSP90 and HDAC, Eur. J. Med. Chem. 150 (2018) 667–677.

[12] V. Certal, J.-C. Carry, F. Halley, A. Virone-Oddos, F. Thompson, B. Filoche-Rommé, Y. El-Ahmad, A. Karlsson, V. Charrier, C. Delorme, A. Rak, P.-Y. Abecassis, C. Amara, L. Vincent, H. Bonnevaux, J.-P. Nicolas, M. Mathieu, T. Bertrand, J.-P. Marquette, N. Michot, T. Benard, M.-A. Perrin, O. Lemaitre, S. Guerif, S. Perron, S. Monget, F. Gruss-Leleu, G. Doerflinger, H. Guizani, M. Brollo, L. Delbarre, L. Bertin, P. Richepin, V. Loyau, C. Garcia-Echeverria, C. Lengauer, L. Schio, Discovery and optimization of pyrimidone indoline amide PI3Kβ inhibitors for the treatment of phosphatase and tensin homologue (PTEN)-deficient cancers, J. Med. Chem. 57 (2014) 903–920.

[13] J.-Y. Chang, H.-P. Hsieh, C.-Y. Chang, K.-S. Hsu, Y.-F. Chiang, C.-M. Chen, C.-C. Kuo, J.-P. Liou, 7-Aroyl-aminoindoline-1-sulfonamides as a novel class of potent antitubulin agents, J. Med. Chem. 49 (2006) 6656–6659.

[14] J.M. Axten, J.R. Medina, Y. Feng, A. Shu, S.P. Romeril, S.W. Grant, W.H.H. Li, D.A. Heerding, E. Minthorn, T. Mencken, C. Atkins, Q. Liu, S. Rabindran, R. Kumar, X. Hong, A. Goetz, T. Stanley, J.D. Taylor, S.D. Sigethy, G.H. Tomberlin, A.M. Hassell, K.M. Kahler, L.M. Shewchuk, R.T. Gampe, Discovery of 7-Methyl-5-(1-{[3-(trifluoromethyl)phenyl]acetyl}-2,3-dihydro-1H-indol-5-yl)-7H-pyrrolo[2,3-d] pyrimidin-4-amine GSK2606414), a Potent and Selective First-in-Class Inhibitor of Protein Kinase R (PKR)-like Endoplasmic Reticulum Kinase (PERK), J. Med. Chem. 55 (2012) 7193–7207.

[15] M.-J. Lai, R. Ojha, M.-H. Lin, Y.-M. Liu, H.-Y. Lee, T.E. Lin, K.-C. Hsu, C.-Y. Chang, M.-C. Chen, K. Nepali, J.-Y. Chang, J.-P. Liou, 1-Arylsulfonyl indoline-benzamides as a new anti agents, with inhibition of histone deacetylase, Eur. J. Med. Chem. 162 (2019) 612–630.

[16] S. Mehndiratta, Y.-F. Chiang, M.-J. Lai, H.-Y. Lee, M.-C. Chen, C.-C. Kuo, C.-Y. Chang, J.-Y. Chang, J.-P. Liou, Concise syntheses of 7-anilino-indoline-N-benzenesulfonamides as antimitotic and vascular disrupting agents, Bioorg. Med. Chem. 22 (2014) 4917–4923.

[17] A. Yacovan, R. Ozeri, T. Kehat, S. Mirilashvili, D. Sherman, A. Aizikovich, A. Shitrit, E. Ben-Zeev, N. Schutz, O. Bohana-Kashtan, A. Konson, V. Behar, O.M. Becker, 1-(sulfonyl)-5-(arylsulfonyl)indoline as activators of the tumor cell specific M2

[18] R. Saxena, G. Gupta, M. Manohar, U. Debnath, P. Popli, Y.S. Prabhakar, R. Konwar, S. Kumar, A. Kumar, A. Dwivedi, Spiro-oxindole derivative 5-chloro-4′,5′-diphenyl-3′-(4-(2-(piperidin-1-yl) ethoxy) benzoyl) spiro[indoline-3,2′-pyrrolidin]-2-one triggers apoptosis in breast cancer cells via restoration of p53 function, Int. J. Biochem. Cell Biol. 70 (2016) 105–117.

[19] Y. Li, Y. Xiong, G. Zhang, L. Zhang, W. Yang, J. Yang, L. Huang, Z. Qiao, Z. Miao, G. Lin, Q. Sun, T. Niu, L. Chen, D. Niu, L. Li, S. Yang, Identification of 5-(2,3-dihydro-1H-indol-5-yl)-7H-pyrrolo[2,3-d]pyrimidin-4-amine derivatives as a new class of receptor-interacting protein kinase 1 (RIPK1) inhibitors, which showed potent activity in a tumor metastasis model, J. Med. Chem. 61 (2018) 11398–11414.

[20] Y. Sasaki, M. Tamura, R. Koyama, T. Nakagaki, Y. Adachi, T. Tokino, Genomic characterization of esophageal squamous cell carcinoma: insights from next-generation sequencing, World J. Gastroenterol. 22 (2016) 2284–2293.

[21] T. Kojima, T. Doi, Immunotherapy for esophageal squamous cell carcinoma, Current Oncology Reports 19 (2017) 33.

[22] O.B. Poyrazoglu, A.C. Dulger, B.S. Gultepe, Helicobacter Pylory infection in patients with esophageal squamous cell carcinoma, Clinics (Sao Paulo, Brazil) 72 (2017) 150–153.

[23] J. Ferlay, I. Soerjomataram, R. Dikshit, S. Eser, C. Mathers, M. Rebelo, D.M. Parkin, D. Forman, F. Bray, Cancer incidence and mortality worldwide: sources, methods and major patterns in GLOBOCAN 2012, Int. J. Cancer 136 (2015) E359–E386.

[24] A. Khvorova, J.K. Watts, The chemical evolution of oligonucleotide therapies of clinical utility, Nat. Biotechnol. 35 (2017) 238–248.

[25] H. Ohnuma, Y. Sato, N. Hayasaka, T. Matsuno, C. Fujita, M. Sato, T. Osuga, M. Hirakawa, K. Miyanishi, T. Sagawa, K. Fujikawa, M. Ohi, Y. Okagawa, Y. Tsuji, M. Hirayama, T. Ito, T. Nobuoka, I. Takemasa, M. Kobune, J. Kato, Neoadjuvant chemotherapy with docetaxel, nedaplatin, and fluorouracil for resectable esophageal cancer: a phase II study, Cancer Sci. 109 (2018) 3554–3563.

[26] M.I. Shahin, J. Roy, M. Hanafi, D. Wang, U. Luesakul, Y. Chai, N. Muangsin, D.S. Lasheen, D.A. Abou El Ella, K.A. Abouzid, N. Neamati, Synthesis and biological evaluation of novel 2-oxo-1,2-dihydroquinoline-4-carboxamide derivatives for the treatment of esophageal squamous cell carcinoma, Eur. J. Med. Chem. 155 (2018) 516–530.

[27] R.Z. Morsi, R. Hage-Sleiman, H. Kobeissy, G. Dbaibo, Noxa: role in cancer pathogenesis and treatment, Curr. Cancer Drug Targets 18 (2018) 914–928.

[28] E. Oda, R. Ohki, H. Murasawa, J. Nemoto, T. Shibue, T. Yamashita, T. Tokino, T. Taniguchi, N. Tanaka, Noxa, a BH3-only member of the Bcl-2 family and candidate mediator of p53-induced apoptosis, Science 288 (2000) 1053–1058.

[29] D.-J. Fu, R.-H. Zhao, J.-H. Li, J.-J. Yang, R.-W. Mao, B.-W. Wu, P. Li, X.-L. Zi, Q.-Q. Zhang, H.-J. Cai, S.-Y. Zhang, Y.-B. Zhang, H.-M. Liu, Molecular diversity of phenothiazines: design and synthesis of phenothiazine–dithiocarbamate hybrids as potential cell cycle blockers, Mol. Diversity 21 (2017) 933–942.

[30] S.-Y. Zhang, D.-J. Fu, X.-X. Yue, Y.-C. Liu, J. Song, H.-H. Sun, H.-M. Liu, Y.-B. Zhang, Design, synthesis and structure-activity relationships of novel chalcone-1,2,3-triazole-azole derivates as antiproliferative agents, Molecules 21 (2016) 653.

[31] D.J. Fu, J.F. Liu, R.H. Zhao, J.H. Li, S.Y. Zhang, Y.B. Zhang, Design and antiproliferative evaluation of novel sulfanilamide derivatives as potential tubulin polymerization inhibitors, Molecules 22 (2017) 1470.

[32] D.-J. Fu, P. Li, J. Song, S.-Y. Zhang, H.-Z. Xie, Mechanisms of synergistic neurotoxicity induced by two high risk pesticide residues – chlorpyrifos and Carbofuran via oxidative stress, Toxicol. In Vitro 54 (2019) 338–344.

[33] D.J. Fu, Y.H. Hou, S.Y. Zhang, Y.B. Zhang, Efficient click reaction towards novel sulfonamide hybrids by molecular hybridization strategy as antiproliferative agents, J. Chem. Sci. 130 (2018) 6.

[34] S.T. Gao, G.S. Tang, D.W. Hua, R.H. Xiong, J.Q. Han, S.H. Jiang, Q.L. Zhang, C.B. Huang, Stimuli-responsive bio-based polymeric systems and their applications, J. Mater. Chem. B 7 (2019) 709–729.

[35] M.M. Zhu, J.Q. Han, F. Wang, W. Shao, R.H. Xiong, Q.L. Zhang, H. Pan, Y. Yang, S.R.K. Samal, F. Zhang, C.B. Huang, Electrospun nanofibers membranes for effective air filtration, Macromol. Mater. Eng. 302 (2017) 1600353–1600380.

[36] D. Lv, M.M. Zhu, Z.C. Jiang, S.H. Jiang, Q.L. Zhang, R.H. Xiong, C.B. Huang, Green electrospun nanofibers and their application in air filtration, Macromol. Mater. Eng. 303 (2018) 1800336–1800354.